https://doi.org/10.5194/egusphere-2025-1402
Preprint. Discussion started: 8 April 2025

Mercury contamination in staple crops impacted by Artisanal Small-scale Gold Mining (ASGM): Stable Hg isotopes demonstrate dominance of atmospheric uptake pathway for Hg in crops.

Excellent O. Eboigbe[1], Nimelan Veerasamy[1], Abiodun M. Odukoya[2], Nnamdi C. Anene[3], Jeroen E. Sonke[4], Sayuri Sagisaka Méndez[5], David S. McLagan[1,6,*]

[1]Dept. of Geological Sciences and Geological Engineering, Queens University, 36 Union St, Kingston ON, Canada, K7L3N6; [2]Department of Geosciences, University of Lagos, G97X+XJC, Yaba, Oworonshoki 101245, Lagos, Nigeria; [3]Ministry of Solid Minerals Development, Government of Nigeria, P.M.B. 107, Luanda Crescent, Wuse II, Abuja 904101, Federal Capital Territory, Nigeria; [4]Géosciences Environnement Toulouse, CNRS/IRD/University of Toulouse, 14 Av. Edouard Belin, 31400 Toulouse, France; [5]Department of Environmental Sciences, University of Toronto, 1265 Military Trail, Toronto, ON, M1C1A4, Canada; [6]School of Environmental Studies, Queen's University, 116 Barrie St, Kingston, ON, K7L3N6, Canada.

* Contact author: david.mclagan@queensu.ca.

Summary

High mercury concentrations are observed in cassava, maize, and peanuts (groundnuts) near an ASGM site. Stable Hg isotopes indicate atmospheric uptake (foliar assimilation) is the dominant mercury uptake mechanism and transfer pathway to other crop tissues in these unsaturated soil crops.

Abstract

This study investigates mercury (Hg) biogeochemical cycling and Hg uptake mechanisms in three common staple crops at a contaminated farm (Farm1) ≈500m from an artisanal and small-scale gold mining (ASGM) processing site (PS) and a background farm (Farm2; ≈8km upwind) in Nigeria. We examine air, soil, and various crop tissues using total Hg (THg), Hg stable isotope, Hg speciation, and methyl-Hg (MeHg) analyses. Results show elevated gaseous elemental Hg (GEM) levels in the air (mean concentrations: 1200 ± 400 ng m^{-3}) and soil (mean THg concentration: 2470± 1640 µg kg^{-1}) at the PS, significantly higher than those at Farm1 (GEM: 54 ± 19 ng m^{-3}; THg: 76.6 ± 59.7 µg kg^{-1}), which are in turn significantly higher than background site, Farm2 (GEM: 1.7 ng m^{-3}; THg: 11.3 ± 8 µg kg^{-1}). These data confirm the ASGM-derived Hg contamination at the PS and the exposures of crops at

https://doi.org/10.5194/egusphere-2025-1402
Preprint. Discussion started: 8 April 2025

Farm1 to elevated levels of Hg in both air and soil. Aligning with Hg concentrations in air and soil, Farm1 had significantly high THg concentration in all crop tissues compared to Farm2. At Farm1, foliage exhibits the highest THg concentrations in tissues across all crops (up to 385 ± 20 μg kg^{-1} in peanuts). These data, along with highly negative $\delta^{202}Hg$ values in foliage and other crop tissues (indicative of light Hg isotope enrichment imparted during stomatal assimilation of Hg) demonstrate atmospheric uptake of GEM as the primary uptake pathway for Hg in these crops. We observe air-to-foliage mass dependent enrichment factors ($\varepsilon^{202}Hg$) of -2.60±0.35, -2.54±0.35, and -1.28±0.43‰ for cassava, peanuts, and maize, respectively. While our two-endmember mixing model shows Hg in crop roots is influenced by both soil (59-74%) and atmospheric (26-41%) uptake pathways, we suggest soil Hg in roots is largely associated with root epidermis/cortex (external root tissues) and little soil derived Hg is transferred to above ground tissues (<7% across all crops). The lower THg concentrations in edible parts (with the exception of cassava leaves, commonly eaten in Nigeria) indicate that even translocation from foliage to other tissues is a relatively slow process. MeHg concentrations were <1% across all tissues and probable dietary intakes (PDI) for both MeHg and THg based on typical diets in Nigeria are all below reference dose thresholds, indicating these crops are low health risk to the local population.

1 Introduction

Artisanal and small-scale gold mining (ASGM) is generally defined as mining activities related to the extraction of gold that involves minimal (or no) mechanisation undertaken by individuals or small groups/cooperatives whose participation in these activities ranges from regulated to informal (illegal); specific definitions can vary between jurisdictions (Hentschel et al., 2002; Seccatore et al., 2014). In recent years, the ASGM sector has grown exponentially, driven by rising gold prices and the ease of selling gold (World Gold Council, 2019; Verbrugge and Geenen, 2019; Achina-Obeng and Aram, 2022). Currently, ASGM contributes ≈20-30% of global gold production (PlanetGOLD, 2022), especially in emerging economies where it serves as a vital source of livelihood for many communities. Despite attempts to regulate mercury (Hg) use in ASGM under the Minamata Convention (UNEP, 2013), elemental Hg (Hg(0)) use remains a fundamental part of gold processing in ASGM due to the effectiveness and simplicity of the Hg-gold amalgamation process (Viega et al., 2006; Bugmann et al., 2022) and the general preference of miners for Hg-amalgamation (Hinton, 2003; Jønsson et al., 2013).

https://doi.org/10.5194/egusphere-2025-1402
Preprint. Discussion started: 8 April 2025

ASGM is now considered the largest global source of anthropogenic Hg emissions (Streets et al., 2019; Munthe et al., 2019; Yoshimura et al., 2021). Recent estimates suggest that ASGM emits 838 ± 163 Mg of Hg to air (almost entirely as gaseous Hg(0): GEM) and releases 1221±637 Mg of inorganic Hg forms, Hg(0) and divalent Hg (Hg(II)) to land and rivers annually (Munthe et al., 2019). The continued rapid growth of the sector in the decade since the ratification and implementation of the Minamata Convention raises questions about the effectiveness of the measures introduced by the Convention in reducing the use and impacts of Hg in ASGM. Such concerns are largely driven by growth in illegal mining, a thriving illicit, international trade market of Hg, and the criminal networks tied to both issues (Verité, 2016; UNEP, 2017; Lewis et al., 2019; Marshall et al., 2020; Cheng et al., 2022). These security issues also present a major barrier to the implementation of more effective and holistic study of Hg use and impacts in ASGM areas (Moreno-Brush, 2021).

GEM has a long atmospheric residence time (≈6-18 months), and long-range atmospheric transport is the dominant mechanism for the global redistribution of Hg (Ariya et al., 2015). Hence, Hg emitted from sources such as ASGM can have impacts on human and environmental health in areas great distances from these activities (Bose-O'Reilly et al., 2010; Weinhouse et al., 2021). Work in recent decades has shown that terrestrial plants play a critical role in the global Hg cycle, acting as the primary sink of atmospheric Hg in terrestrial systems through the assimilation of GEM into foliar stomata during photosynthesis (a mechanism of GEM dry deposition) and subsequent storage within plant tissues (Jiskra et al., 2018; Obrist et al., 2021). This is observed in trees, grasses (e.g. Millhollen et al., 2006; Mao et al., 2013; Assad et al., 2016), and crops like rice, wheat, and corn (e.g. Niu et al., 2011; Yin et al., 2013; Sun et al., 2019). Total Hg (THg) concentrations in plant foliage (and other above ground tissues) are proportional to local GEM concentrations (Millhollen et al., 2006; Fu et al., 2016; Sun et al., 2019; Wang et al., 2020). Another potential uptake pathway of atmospheric Hg in plants is sorption to and transfer through the foliage cuticle. Yet wash-off by precipitation, revolatilisation of sorbed Hg, and the likely slow transfer through the cuticle result in this uptake mechanism being minor compared to the stomatal assimilation pathway (Rea et al., 2000; Rutter et al., 2011a; 2011b; Laacouri et al., 2013). While there is potential for plants to also take up Hg from soil via roots, a large body of research indicates that >90% of Hg in the above-ground biomass of plants is derived from the air-foliage pathway with the root epidermis/cortex providing an effective barrier for the less bioavailable forms of Hg found in soils (Beauford et al., 1977; Rutter et al., 2011b; Zhou et al., 2021). A major exception to this is the uptake of the more bioaccumulative and toxic methyl-Hg (MeHg) in species growing in saturated soils such as rice (Qui et al., 2007).

https://doi.org/10.5194/egusphere-2025-1402
Preprint. Discussion started: 8 April 2025

Critical to the advancements that have been made in understanding the importance of this GEM uptake mechanism by vegetation is the use of Hg stable isotope analyses in air, plants, soils, and precipitation samples. Hg has seven stable isotopes, which undergo both mass-dependent fractionation (MDF) and mass-independent fractionation (MIF) in the environment (Blum and Bergquist, 2007). MDF occurs during biogeochemical transformations, while processes causing MIF are rarer and linked largely to photochemical processes and some dark abiotic reactions; both MDF and MIF enable researchers to track Hg sources and identify *in-situ* transformation processes (Bergquist and Blum, 2009). For example, MDF is useful in tracking plant uptake, where foliage often shows large negative MDF shifts (-1 to -3 ‰ in δ^{202}Hg) during stomatal assimilation compared to the δ^{202}Hg isotope values of GEM in the surrounding air (Zhou et al., 2021, and references therein). After being taken up by leaf stomata, GEM is rapidly oxidised to divalent forms and can then translocate to other plant tissues, including stems, branches, bark, and seeds, supported by negative δ^{202}Hg values in stem and seeds that closely resemble values of observed in foliage (Yin et al., 2013; Sun et al., 2019; Liu et al., 2020; McLagan et al., 2022a).

Significant gaps remain in our understanding of Hg uptake mechanisms, internal cycling, and associated health risks from Hg in crops particularly as this relates to the largest global anthropogenic emitter of Hg: ASGM. The limited number of studies examining Hg in crops affected by ASGM activities have primarily focussed on THg and occasionally also MeHg analyses, which may not fully capture the complexity of Hg dynamics in these systems. In addition, such studies have typically assumed soil-roots as the dominant Hg uptake mechanism (Suhadi et al., 2021; Addai-Arhin et al., 2023).

In this study, we employ a multidisciplinary, total systems approach to comprehensively examine the dominant Hg uptake pathway, and internal translocation and storage of Hg in three staple crops in a Nigerian farm adjacent to ASGM activities. Air, soil, and a range of crop tissues (foliage, stems, roots, and tubers/grains) were assessed using a series of Hg analyses (THg, MeHg, Hg stable isotopes, and Hg speciation) to provide critical data on the biogeochemical cycling of Hg in agricultural regions impacted by ASGM and preliminary assessment of the potential risks to human health from consuming these crops.

2 METHODS

https://doi.org/10.5194/egusphere-2025-1402
Preprint. Discussion started: 8 April 2025

We note, methods described in this section are abbreviated due the need for conciseness and to the broad multidisciplinary approach utilised. Full details of the study site, sampling approaches, analytical methods, and quality assurance and quality control (QAQC) are provided in the supplementary information.

2.1 Study Area

The study is based around a mine (8.87126° N, 7.71828° E) and ASGM processing site (8.9012° N, 7.7061° E) separated by ≈3.5 km and situated near the town of Uke (population: ≈20,000) in the Karu Local Government Area of Nasarawa State, ≈51 km southeast of Abuja, the capital city of Nigeria (Figure 1). ASGM in this area began around 2015 following the discovery of gold, which attracted a significant influx of miners and includes mining, ore processing with Hg, and amalgam burning (further details of the ASGM activities are described in Section S1).

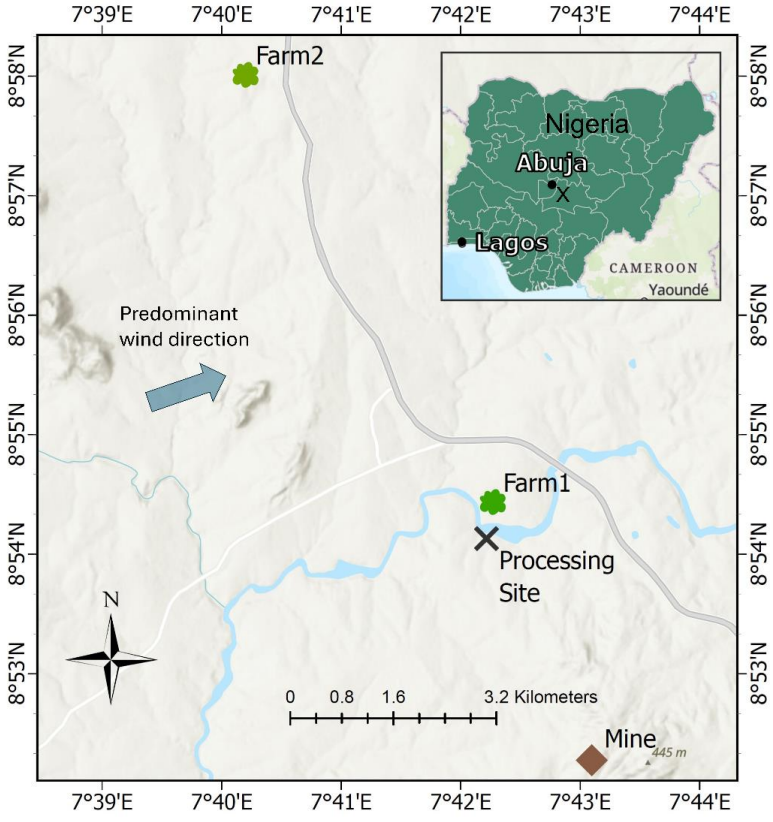

Figure 1: Map showing the study area showing mine, processing site (PS), Farm1, Farm2,

https://doi.org/10.5194/egusphere-2025-1402
Preprint. Discussion started: 8 April 2025

predominant winds in the region (Lorhemba and Mijinyawa, 2021), and an inset map indicating site and major Nigerian cities and the processing site marked by the 'x' (Basemap: ©OpenStreetMap Foundation).

In July 2023, sampling was conducted at three sites: (1) the ASGM processing site (Site name: PS), (2) Farm1: situated ≈0.5 km north of the processing site, and (3) Farm2: a control farm located ≈8 km north-northwest of the processing site in another town with no known sources of Hg, ASGM or otherwise (Figure 1). Predominant winds in this region are from the west-southwest (Iorhemba and Mijinyawa, 2021); thus, there is potential for emissions from the processing site to impact Farm1 (but unlikely to influence Farm2). Critically, Farm1 is on the opposite side to the processing site to ensure surface or groundwater flows from the processing site were not contaminating the Farm1 soils. We note that the informal nature of ASGM restricted sampling to the scope outlined below, and this was by invitation and allowable concession of the operators of the legally operating site, local and national governmental authorities, and the farmers themselves. This was particularly limiting to the number Hg stable isotope samples that could be collected for each crop and crop tissue type.

2.2 Soil sampling

Surface soil samples (0 – 10 cm) were collected from the PS (n=13), Farm1 (n=8), and Farm2 (n=5) (farm soils were sampled directly around sampled plants) using standard sampling procedures (USEPA, 2023). Full details of the soil sampling procedures are provided in Section S2.

2.3 Air sampling

Considering the substantial emissions of Hg to air from ASGM and the potential for GEM uptake by vegetation (crops), it was critical to assess GEM concentrations. Hg passive air samplers (MerPAS; Tekran Instruments Corp.) were deployed according to the guidelines of the developers (McLagan et al., 2016), and modifications were made for deployments in highly contaminated areas (shorter deployments and extreme care in sampler transport and storage) (McLagan et al., 2019; Tekran Instruments, 2020; Si et al., 2020). MerPAS were deployed for ≈72 hours as PS (n=3), ≈144 hours at Farm1 (n=6), and ≈100 days at (control) Farm2 (n=1). See Section S2 for full details on MerPAS deployments (including blank details) and Table S7.1 for specific sampling periods.

2.4 Crop sampling

Foliage, stem, grains/tubers, and roots samples of three crops cultivated in both Farm1 and Farm2:

https://doi.org/10.5194/egusphere-2025-1402
Preprint. Discussion started: 8 April 2025

maize (*Zea mays*), cassava (*Manihot esculenta*), and peanuts (*Arachis hypogaea*) were collected. We note that in cassava, tubers are true roots, but we classify "roots" as undeveloped (no tuber) adventitious roots/rootlets (Rees et al., 2012). Cassava and maize were nearing maturity at the time of sampling and ≈1-2 months (or less) before harvest, while peanuts were fully mature and being harvested at the time of sampling. Three whole plants of each crop at each farm were removed from the soil for sampling with care made to consolidate below ground tissues with each selected plant. Due to sampling availability and access restrictions placed by farmers, the community, and mine owners we could not deviate from this sample timing (and quantity). Full Details of crop sampling procedures are provided in Section S2.

2.5 Analytical Procedures

2.5.1 Solid-phase THg analyses

THg analysis for soil and plant samples (0.01 – 0.2 g aliquots) was carried out by thermal desorption, gold amalgamation, and atomic adsorption spectrometry according to USEPA Method 7473 (USEPA, 2007) using a MA-3000 direct Hg analyser (Nippon Instruments Corp.). All tissue and soil samples were measured in triplicate for THg and full details of the analytical method are provided in Section S3. THg concentration analysis of MerPAS samples also utilised the MA-3000 Direct Hg Analyser (with ≈0.1 g additions of pre-cleaned sodium carbonate) and followed methods developed by McLagan et al. (2016) with some refinements (including a verified 400°C maximum combustion temperature) detailed in Section S3. Calculations of GEM concentrations (ng m^{-3}) followed methods described by McLagan et al. (2016) and further details are provided in Section S3. MerPAS samples used for Hg stable isotope analyses of GEM were corrected for the MDF offset (measured δ^{202}Hg +1.1 ± 0.2 ‰) as posited by Szponar et al. (2020).

Quality assurance and quality control (QAQC) were exercised using replication of all THg sample analyses (2-3 replicates), and regular (after every 10 sample runs) analyses of (matrix matched) certified reference materials (CRMs) and the internal liquid Hg standard. All recoveries were within accepted ranges and specific details on the CRMs used and recovery data are presented in Table S3.1. All data are presented on a dry-weight (dw) basis.

2.5.2 Hg stable isotopes: extractions and analyses

All samples analysed for Hg stable isotopes were trapped off the exhaust of the MA3000 detector

https://doi.org/10.5194/egusphere-2025-1402
Preprint. Discussion started: 8 April 2025

during solid-phase THg analyses of the same matrix. The combust and trap method broadly followed methods by Enrico et al. (2021) and McLagan et al. (2022b) with some modifications. This method allows accumulation of Hg from matrix matched samples measured for solid-phase THg concentrations within a single 5 or 10 mL inverse aqua regia (3:1 concentrated HNO_3:HCl diluted to 40% v/v with DI water) trap. MA-3000 combustion method followed the matrix specific methods described in Section S3. A heated (≈60 °C) polytetrafluoroethylene (PTFE) tube connected a coarse frit gas dispersion sparger (6 mm outer diameter; modified to 25 cm length) was connected to the MA-3000 detector outlet. Trapping samples analysed for THg concentrations allows for direct recovery testing between the measured THg solid-phase concentrations to the liquid-phase THg concentrations within the trap, which removes the uncertainty of assuming homogenous THg solid-phase concentrations. Any sample with recovery below 80% was not considered for Hg stable isotope analyses due to concerns that losses during extraction/analyses could artificially induce isotope fractionations. Recoveries of all samples analysed for Hg stable isotopes are listed in Table S3.3. All samples were diluted to a 20% acid strength (by volume) for Hg stable isotope analyses.

An online cold vapor generator (CETAC-HGX-200) was used to reduce Hg(II) in the trapping solutions into Hg(0) vapor by $SnCl_2$ (3% w/v in 1 M HCl). Using this system, gas-phase Hg(0) is then introduced into a multi-collector inductively coupled mass spectrometry (MC-ICP-MS, Thermo-Finnigan Neptune) for analyses of Hg stable isotopes at the Observatoire Midi-Pyrenees (Toulouse, France). Full details of instrument setup can be found in Sun et al., 2013. Sample isotope ratios were corrected for mass bias by sample-standard bracketing using NIST 3133 (Blum and Bergquist, 2007; Sun et al., 2013). Results are reported as δ-values in per mil (‰) by referencing to NIST 3133, representing Hg mass-dependent fractionation (MDF), while MIF is reported in "capital delta" notation (Δ), which is the difference between the measured values and those predicted by the kinetic MDF law using equations previously stated (Blum and Bergquist, 2007). The quality control of Hg isotope measurements was assessed by analysing ETH-Fluka, and UM Almaden reference standards and these data are presented in Table S3.3. Uncertainties on sample δ and Δ-signatures were conservatively estimated as the larger of the 2 standard deviation uncertainties on weekly ETH-Fluka, UM-Almaden or sample replicates (Table S3.3).

2.5.3 Hg Speciation Analyses

Solid-phase speciation was performed using the pyrolytic thermal desorption (PTD) method developed by Biester and Scholz (1996) adapted for use on a Lumex 915M with PYRO-915+ Module

https://doi.org/10.5194/egusphere-2025-1402
Preprint. Discussion started: 8 April 2025

(Lumex Instruments Corp.) by Mashyanov et al. (2017). Due to the inherent uncertainties and challenges in peak identification of Hg(II) species, these analyses are considered qualitative and complementary (McLagan et al., 2022b). Further details of this method are provided in Section S3.

2.5.4 Methyl-Hg (MeHg) Analyses

MeHg concentrations were determined using isotope dilution method and followed methods described in Mitchell and Gilmour (2008). A detailed description of this method is provided in Section S3. All QAQC data for MeHg analyses are presented in Table S3.2.

2.6 Two endmember mixing model to identify Hg sources within crops

A two-endmember mixing model using the (1) δ^{202}Hg values of foliage for each crop and (2) the mean δ^{202}Hg value for Farm1 soils was used to quantitatively determine source pathways for Hg in internal crop tissues according to Equation S4.1 (Section S4).

2.7 Estimates of annual Hg dry deposition rates to crops

Hg(0) dry deposition rates ($F_{Hg(0):AGB}$; g km^{-2}) via the foliar uptake pathway to the aboveground biomass (AGB) for each crop were calculated using Equations S5.1 and S5.2 adapted from Casagrande et al. (2020) with additions relating to the transfer of Hg to other above ground tissues and the transfer to edible below ground parts (for peanuts and cassava). This was achieved using annual edible biomass yields and the fraction of Hg in tubers/nuts derived from a foliage-based two-endmember mixing model (Table 1). Details of these calculations are provided in Section S5.

2.8 Probable daily intake calculations

We also calculated the probable daily intake (PDI) of MeHg and Hg(II) using the method from Zhao et al. (2019) adapted for MeHg and Hg(II) and the concentrations measured in the examined crops and their mean dietary intake data for adults in Nigeria. Specific equations and data used in these calculations and the PDI data generated are presented in Section S6.

2.9 Statistical Analyses

Statistical tests (Welch's T-test; unequal variances and sample sizes) used to assess differences in THg concentrations and Hg stable isotopes, data analyses, and figure generations were all generated in R-Studio (Boston, USA).

https://doi.org/10.5194/egusphere-2025-1402
Preprint. Discussion started: 8 April 2025

3 Results and Discussion

3.1 Crop exposure levels: Hg concentrations in air and soils

Highly elevated GEM concentrations (1200 ± 400 ng m^{-3}) were observed at the ASGM processing site (PS) (Figure 2). These concentrations are ≈1000x background concentrations and consistent with levels observed in other ASGM regions where Hg is used in ASGM activities (González-Carrasco et al., 2011; Kawakami et al., 2019; Nakazawa et al., 2021; Snow et al., 2021) and indicate substantial Hg use and emissions at PS. At Farm1 (≈500m distance from PS), GEM concentrations were significantly lower than at PS (p=0.014), but remained elevated (54 ± 19 ng m^{-3}) above background, confirming exposure of Farm1 to GEM emissions from ASGM activities at PS. In contrast, GEM concentrations at Farm2 (1.7 ng m^{-3}, n=1) were consistent with the Northern Hemisphere background concentrations (≈1.5 – 2 ng m^{-3}; Sprovieri et al., 2016).

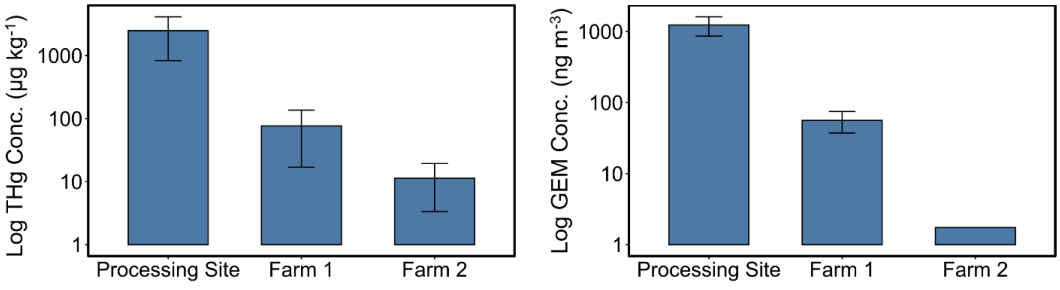

Figure 2: THg concentrations in soils (left; µg kg^{-1}) and GEM concentrations in air (right; ng m^{-3}) for all sampling sites.

Stable isotope measurements of GEM at sites exposed to elevated GEM concentrations were indicative of more negative MDF and more positive MIF signatures (PS: δ^{202}Hg: -1.38 ± 0.21 ‰, Δ^{199}Hg: 0.07 ± 0.03 ‰; Farm1: δ^{202}Hg: -0.94 ± 0.19 ‰, Δ^{199}Hg: 0.08 ± 0.08 ‰) (Figure 4), which is typical of anthropogenic Hg emitted into air from industrial (Sonke et al., 2010; Fu et al., 2021; McLagan et al., 2022b) and ASGM (Gerson et al., 2022; Szponar et al., 2025) sources. Contrastingly, GEM at Farm2 was relatively enriched in heavier isotopes and had a slightly negative MIF signal (δ^{202}Hg: -0.01 ± 0.19 ‰; Δ^{199}Hg: -0.12 ± 0.08 ‰) typical for GEM samples in background areas (Si et al., 2020; Szponar et al., 2020). We suspect that the rapid decline in GEM concentrations as we move away from the contamination source is influenced both by dilution with background air and by wind direction. Although GEM was not measured in areas downwind of the processing site, McLagan et al. (2019)

https://doi.org/10.5194/egusphere-2025-1402
Preprint. Discussion started: 8 April 2025

observed a more gradual decline in GEM in areas downwind (compared to upwind sites) of a former Hg mine that remained heavily contaminated by elemental Hg; we suggest a similar pattern is likely at our study site. The vegetation of the area itself may play a role in reducing GEM concentrations around the ASGM area by removing GEM from the atmosphere during plant growing seasons. An assessment of this flux is described below in Section 3.4.

Similar to GEM, soil samples at PS were heavily contaminated (mean THg concentration:2470 ± 1640 μg kg^{-1}). Elevated soil Hg at the processing site is likely due to rapid GEM deposition from the atmosphere after emissions from amalgam burning and direct spills from improper handling of liquid Hg (Telmer and Viega, 2009). The large variation in soil THg concentrations at this site (see Table S4.1) also reflects the spatial heterogeneity of processing activities at PS where Hg-Au amalgamation, ore washing, amalgam burning, and other activities occur.

Farm1 soils were also contaminated (mean THg concentration: 80.9 ± 60.1 μg kg^{-1}), but similar to differences in GEM concentrations, Farm1 was 1-2 orders of magnitude (and significantly; $p<0.001$) lower than PS ≈500m away. Hence, we suggest emissions of GEM from the PS and deposition directly to soils or via GEM assimilation into vegetation, litterfall, and decomposition as the dominant contamination pathway at Farm1, a mechanism now well described in the literature (Jiskra et al., 2015; Obrist et al., 2017; Zhou and Obrist, 2021). Our results fall into the range of concentration (2 – 5570 μg kg^{-3}) recorded by Odukoya et al. (2020) from farmlands adjacent to an ASGM region in Niger state of Nigeria and farms impacted by ASGM in Brazil (81.7 ± 13.5 μg kg^{-1}) (Casagrande et al., 2020). The latter study by Casagrande et al. (2020), is one of the only other studies examining Hg in ASGM impacted agricultural areas directly attributing elevated concentrations in farm plants and soils to the atmospheric transfer pathway. In contrast, Farm2 soils were significantly lower again than Farm1 (p=0.029) and at background levels with a mean concentration of 11.3 ± 8.0 μg kg^{-1}.

All soil samples exhibited little variation in δ^{202}Hg (PS: 0.29 ± 0.98 ‰; Farm1 -0.26 ± 0.43 ‰) and Δ^{199}Hg MIF signal (PS: -0.09 ± 0.12 ‰; Farm 1 -0.07 ± 0.03 ‰). Nonetheless, the mean Δ^{199}Hg for GEM is slightly (but not significantly; p=0.073) higher than the mean value for soils. This suggests minor evidence of some MIF induced by photochemical reduction from the soils (Rose et al., 2015).

3.2 Hg contamination and distribution in crops grown in ASGM impacted areas

https://doi.org/10.5194/egusphere-2025-1402
Preprint. Discussion started: 8 April 2025

With the confirmation of exposure levels in both air and soils at Farm1 and Farm2 (control), it was then critical to assess the degree to which this contamination is affecting staple crops grown in this area and determine the predominant uptake mechanism of Hg in these plants. The mean THg concentration in peanut (p=0.021), cassava (p=0.015), and maize (p=0.004) tissues were all significantly elevated at Farm1 compared to Farm2 (Figure 3 and Table S4.3). The highest THg concentrations were detected in foliage of peanuts and cassava at Farm1 (peanut: 385 ± 20 μg kg^{-1}; cassava: 320 ± 116 μg kg^{-1}) and Farm2 (peanut: 7.06 ± 2.74 μg kg^{-1}; cassava: 13.2 μg kg^{-1}) (Figure 3), which suggests that the stomatal assimilation pathway is likely the dominant uptake mechanism of Hg in cassava, and peanuts. While foliage THg concentrations were also elevated in maize (Farm1: 182± 44 μg kg^{-1}; Farm2: 5.16 μg kg^{-1}), again demonstrating the likelihood of foliar Hg uptake, concentrations in maize roots were slightly higher (Farm1: 202 ± 136 μg kg^{-1}; Farm2: 5.74 ± 3.73) than foliage. Roots also had the second highest concentration in peanuts and cassava. These data suggest potential for soil-to-root Hg uptake in all three crops, but the contribution of the uptake mechanisms will be examined in more detail in Section 3.3.

Adjorololo-Gasokpoh et al. (2012) measured similar THg in cassava foliage (up to 177 μg kg^{-1}) and tuber (up to 185 μg kg^{-1}). Even though they did not observe any significant trends or differences between tissues, a novel component of their study was the division of cassava tuber into flesh, inner peel, and outer peel (Adjorololo-Gasokpoh et al., 2012). Division of root tissues into epidermis, cortex, and vascular bundle (or stele) and then analysis for THg and stable Hg isotopes in crops impacted by ASGM would provide critical insight into the effectiveness of epidermis and/or cortex in restricting Hg uptake into the vascular bundle of inner root, as has been suggested elsewhere (Rutter et al., 2011b; Lomonte et al., 2020; Yuan et al., 2022).

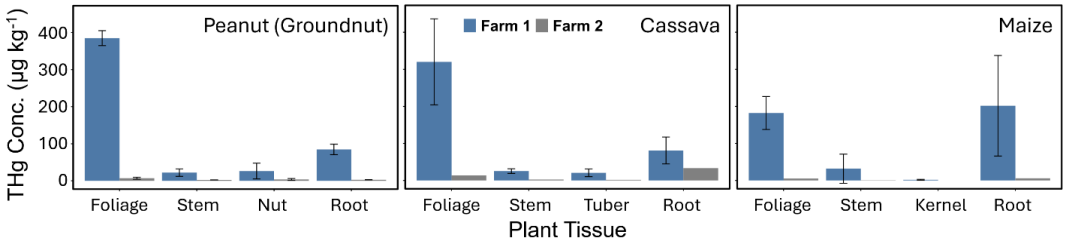

Figure 3: THg concentration (μg kg^{-1}) for all crop tissues at Farm1 and Farm2

Similar results showing the highest crop tissue THg concentrations in ASGM affected farms are common in the literature (i.e., [cassava] Golow and Adzei, 2002; [cassava] Nyanza, et al., 2014; [soy:

https://doi.org/10.5194/egusphere-2025-1402
Preprint. Discussion started: 8 April 2025

Glycine max] Casagrande et al., 2020). However, we note the challenges of comparing absolute THg concentrations even of samples from the same species as distance from ASGM activities is likely a major determinant controlling observed levels of crop contamination and, in many cases, little specific information on source-receptor distances is provided (i.e., Essumang et al., 2007; Adjorololo-Gasokpoh et al., 2012; Nyanza et al., 2014).

Of the three crops we studied, maize foliage exhibited lower THg concentrations than other crops, which may be attributed to maize's C4 photosynthetic pathway. An earlier study by Browne and Fang (1983) found C3 plants to take up five times more atmospheric Hg than C4 species due to differences in leaf surface area, stomatal conductance (C3 plants exchange gases more readily with the atmosphere, allowing for greater uptake of atmospheric Hg), and internal resistance to Hg vapor uptake within the plant. Furthermore, maize kernels (1.78 ± 1.22 μg kg^{-1}) contained the lowest concentration in all crops at Farm1 suggesting minimal translocation from foliage or roots as observed by Wang et al. (2024), which again may be attributable to physiological differences in C4 species – a hypothesis that requires direct exploration in future research. Glauser et al. (2022) also suggest non-stomatal pathways can result in Hg sorption in certain maize tissues such as maize tassels and silk. Although cassava is an intermediate between C4 and C3 plants (exhibiting some properties of both C3 and C4 photosynthetic pathways (El-Sharkawy and Cook, 1987; Bräutigam and Gowik, 2016; Xia et al., 2023), THg concentrations in cassava were higher than those of maize. This phenomenon is, however, not yet fully understood and warrants further research.

The concentration patterns for the crops were as follows: for maize, roots > foliage > stem > kernel; for peanuts, foliage > roots > nut > stem; and for cassava, foliage > roots > stem > tubers. All crops exhibited the lowest concentrations in their edible parts (kernel, nuts and tubers), except for the peanut stem, which was slightly lower than the nuts. This finding aligns with studies on rice in China, where the stem and seeds consistently showed the lowest THg concentrations across all measured sites (Yin et al., 2013).

3.3 Tracing Uptake and Translocation of Hg Within Crops using Hg Stable Isotopes

While THg quantifies the extent of overall Hg exposure in the examined crops, we have thus far neither been able to fully confirm the Hg uptake pathway nor explain translocation processes within the crop. We therefore applied Hg stable isotope analyses to investigate these processes in greater detail.

https://doi.org/10.5194/egusphere-2025-1402
Preprint. Discussion started: 8 April 2025

359 Foliage samples across all crops displayed highly negative MDF values with δ^{202}Hg values being -3.83
360 ± 0.19 ‰ (2SD) for cassava, -3.77 ± 0.19 ‰ (2SD) for peanuts, and -2.51 ± 0.32 ‰ (1SD) for maize
361 (Figure 4). MIF values were all near zero (Δ^{199}Hg range: -0.04 – 0.03 ‰) (Figure 4). Sun et al. (2020)
362 measured similar MDF values in maize foliage (-2.68 ± 0.28 ‰ (1SD). Yet they also observed more
363 negative δ^{202}Hg in higher concentration samples (Sun et al., 2020), which is likely linked to GEM
364 influenced by anthropogenic sources having more negative δ^{202}Hg.

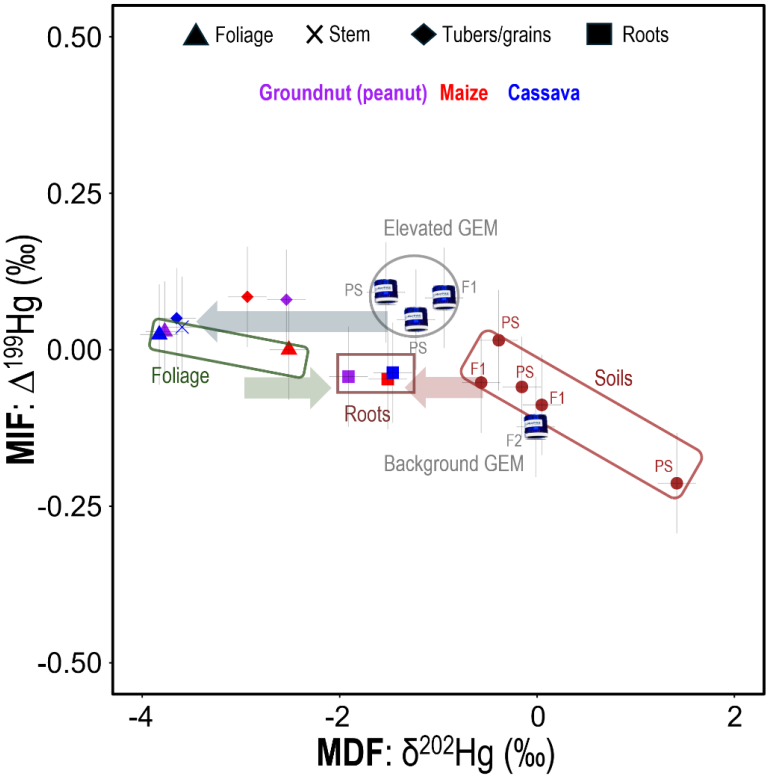

365

366 *Figure 4. MDF (δ^{202}Hg) and MIF (Δ^{199}Hg) for GEM at PS, Farm1 (F1), Farm2 (F2), soil samples at PS and*
367 *Farm1 (F1), and crop tissues for Farm1 (F1) only. The direction of the arrows shows approximate MDF*
368 *from air to foliage (stomatal assimilation; blue arrow), foliage to roots (green arrow), and soil to roots*
369 *(red arrow). Note that cassava tubers are flesh only (no peel).*

370 Assuming all the Hg within foliage for these crops grown in unsaturated soils is derived from stomatal
371 assimilation, we can use the mean Hg stable isotope values for GEM (MerPAS values from both PS
372 and Farm1 to provide estimate variance) to estimate the enrichment factors (indicated by ε for MDF
373 and E for MIF) associated with the stomatal assimilation process for the stomatal assimilation

https://doi.org/10.5194/egusphere-2025-1402
Preprint. Discussion started: 8 April 2025

process in these crops. We calculate ε^{202}Hg for stomatal assimilation to be -2.60 ± 0.35, -2.54 ± 0.35, and -1.28 ± 0.43 ‰ for cassava, peanuts, and maize, respectively, and these data represent the first time such fractionation factors have been calculated for any agricultural crops. These crop stomatal assimilation MDF enrichment factors fall within the range reported (-1 to -3 ‰) in other vegetation (Zhou et al., 2021; Liu et al., 2024; and references therein). There was a small MIF between GEM and foliage (E^{199}Hg: cassava: -0.05 ‰; peanuts: -0.05 ‰; maize: -0.11 ‰), which is similar to the small range observed during this process elsewhere (Demers et al., 2013). The small negative MIF shift can be attributed to minor in-planta photochemical Hg(II) reduction (Demers et al., 2013) and is typically accompanied by an enrichment in the heavy Hg isotopes, and positive shift in δ^{202}Hg; while speculative, this could again be attributable to differing physiological processes (i.e., C4 photosynthesis).

Crop root samples exhibited negative δ^{202}Hg values (cassava: -1.46 ‰; peanuts; -1.91 ‰; maize: ‰) that were distinct from both soil and foliage samples, while Δ^{199}Hg values were similar to those of soil and slightly more negative than GEM and foliage samples (Figure 4). We suggest that the Hg in roots reflects a combination of inputs from both soil and foliage (via stomatal assimilation). Since foliage is a source of energy to plants in the form of the photoassimilates they generate, which are exported to growth (meristems, cambium) and storage (roots, fruits, seeds) tissues via the phloem (Turgeon, 2006), Hg is likely translocated similarly as has been posited in other studies (Zhou et al., 2021; McLagan et al., 2022a). For maize and peanut roots, PTD speciation analysis (see Figure S8.1) revealed the presence of two distinct Hg pools, which we suggest could be representative of distinct fractions of Hg in (i) the epidermis/cortex (likely derived from surrounding soils) and (ii) inner root tissues: vascular bundle/stele (likely derived from air/foliage).

We also apply a two-endmember mixing model using the mean δ^{202}Hg values of (i) GEM at Farm1 and PS, and (ii) soils at Farm1, minus the soil-to-shallow roots (roots above 150cm) MDF (ε^{202}Hg: -0.35) from Yuan et al. (2022), as endmembers to introduce more quantitative assessment of the Hg uptake mechanisms (air/foliage vs soil) (Equation S4.1). Data reveal that between 47% (peanuts) and 66% (cassava) of Hg found in the roots of these crops is derived from air/foliage (Table 1). There is precedence for the transfer of Hg from foliage to roots with a previous study using Hg stable isotopes to indicate 44-83% of Hg in roots is derived from air in selected tree and shrub species (Wang et al., 2020). These data support the hypothesis that the majority of Hg transferred from soil to roots is likely bound to outer root tissue (epidermis/cortex) as suggested elsewhere (Rutter et al., 2011b; Lomonte

https://doi.org/10.5194/egusphere-2025-1402
Preprint. Discussion started: 8 April 2025

et al., 2020). Again, root tissue sectioning and analysis for concentrations and stable Hg isotopes would provide the most conclusive evidence of such processes.

Hg stable isotope data for other crop tissues provided further evidence of translocation of Hg away from foliage. Due to the lower concentration and limited available sample, stems could only be analysed for stable isotopes in cassava, and this one sample displayed almost identical MDF and MIF signatures to cassava foliage (93% derived from air/foliage; Table 1). Edible parts of maize (kernel; 100% from air/foliage) and cassava (tuber flesh; 95% from air/foliage) displayed similar patterns (Table 1). Studies on cassava in ASGM regions, such as those by Nyanza et al. (2014), have similarly demonstrated that Hg concentrations in cassava tubers remain low even in highly contaminated soils, emphasising the influence of foliar pathways. This contrasts with the common assumption that tubers accumulate Hg mainly through soil uptake (Adjorlolo-Gasokpoh et al., 2012).

Table 1: Hg uptake source apportionment in crop tissues using two-endmember, Hg stable isotope mixing model. Foliage is not included as δ202Hg values for foliage represent one of the source endmembers for each crop. All estimates come with a ±16% uncertainty derived from propagating uncertainty terms through calculations.

	Cassava			Maize		Peanut	
Source	Stem	Tuber flesh	Root	Kernel	Roots	Nut	Roots
Air/foliage	93%	95%	26%	100%	47%	61%	41%
Soil/roots	7%	5%	74%	0%	53%	39%	59%

The only exception to this was peanut nuts, which had a δ^{202}Hg value more similar to roots (39% of nut THg derived from soil) and the most positive Δ^{199}Hg value (0.08‰) of any sample across all studied matrices. While we do not have a clear explanation for the anomalous Δ^{199}Hg value of the nut sample, we link the similar δ^{202}Hg values between peanut roots and nuts to the subsurface growth of the nut. Cassava tubers also grow underground, but their physiological function is as a plant energy storage tissue (Rees et al, 2012) as opposed to the peanut nut, which is a seed used for reproduction (Basuchaudhuri, 2022). The transfer of Hg from soils, through peanut shells and into the nut is still somewhat surprising as other studies have shown the shell to be an effective barrier at preventing metal uptake to the nut (Tang et al., 2024) including for Hg (Namasivayam and Periasamy, 1993; Cobbina et al., 2018). Nonetheless, Liu et al. (2010) observed lower Hg adsorption efficiency by natural (compared to chemically modified) peanut shells; though, we note this was in a laboratory study of just shells (nuts removed). Multi-method analyses of peanut shells would be a useful

https://doi.org/10.5194/egusphere-2025-1402
Preprint. Discussion started: 8 April 2025

addition to future work.

3.4 Foliage as an important sink of GEM in ASGM areas

We also used Equations S4.2 and S4.3 to assess the annual GEM dry deposition flux from the atmosphere to these crops via stomatal assimilation. The GEM deposition rates from the atmosphere to leaves for peanuts, maize, and cassava were estimated to be 110±80, 690±130, and 1170±180 g km^{-2} yr^{-1}, respectively. The relatively high GEM deposition rate observed for cassava shows the higher vulnerability of cassava to Hg uptake despite it being grown once annually. This may be due to its larger biomass compared to maize and peanuts. These data were substantially higher than the 13-25 g km^{-2} yr^{-1} estimate for soybeans by Casagrande et al. (2020). While this is partly attributable to Casagrande et al. (2020) not accounting for transfer from foliage to other above or below ground tissues, our estimates were dominated by Hg storage in foliage (90-92% of total; see Table S5.1). Hence, we attribute the differences between the two estimates to differences in distances between ASGM activities and farms/crops, scale of ASGM operations, and different crop physiological uptake mechanisms. These data provide crucial insight into the role of crop foliage in sequestering atmospheric Hg in regions impacted by ASGM and can be useful in environmental monitoring and risk assessment. In regions with ongoing ASGM activities, these estimates could be used as baselines to monitor shifts in atmospheric Hg concentrations over time. For instance, if emissions from ASGM were to decline due to policy interventions, a corresponding reduction in annual Hg deposition rates would be expected. Conversely, if emissions increase, these crops could serve as bioindicators for heightened atmospheric contamination.

3.5 Human health implications

MeHg concentration data is typically considered the major endpoint for assessing human and environmental health impacts of Hg. MeHg concentrations were consistently below 1% of total Hg (THg) in all samples (Table S7.5), suggesting low methylation of Hg(II) in these soils for these crops. Moreover, the probable daily intake (PDI) for MeHg in these crops (<0.001 μg kg^{-1} day^{-1}) or the sum of their dietary intakes (0.0010±0.0016 μg kg^{-1} day^{-1}) are two orders of magnitude below the USEPA reference dose (RfD) for MeHg of 0.1 μg kg^{-1} day^{-1} (USEPA, 2001). This contrasts data from rice grown in Hg contaminated areas, which is known to accumulate MeHg (via root uptake) due to the capacity of rice paddies to host anoxic conditions known to produce this highly bioaccumulative species (Zhao et al., 2016; 2020).

https://doi.org/10.5194/egusphere-2025-1402
Preprint. Discussion started: 8 April 2025

While less toxic than MeHg, inorganic Hg has been associated with health effects on gastrointestinal, renal, and nervous systems (Ha et al., 2017; Basu et al., 2023). Due to the low MeHg concentrations, inorganic Hg exposures were assessed using THg concentrations and these values were adjusted for the lower absorption rates of inorganic Hg (7%; WHO, 1990); this adjustment allows direct comparison of inorganic Hg/THg exposures to the MeHg RfD value (Zhao et al., 2019). While PDI values for inorganic Hg/THg were higher in all edible crop tissues examined (individual crop range: 0.0001 μg kg^{-1} day^{-1} in maize to 0.016 μg kg^{-1} day^{-1} in cassava leaves; dietary sum: 0.023±0.007 μg kg^{-1} day^{-1}; Table S6.1), they are again below the MeHg RfD value. Hence, there is little health risk to the local population from Hg levels ingested during typical consumption of the studied tubers/grains/nuts.

Cassava leaves are commonly consumed in various regions including Nigeria (El-Sharkawy, 2003); hence, the high inorganic Hg in cassava leaves we observed in particular could pose some risk. Without direct data for estimated dietary intake of cassava leaves in Nigeria, we chose to assume a conservative daily intake rate (50 g day^{-1}; Section S6). Latif and Müller (2015), report that cassava leaves are consumed up to 500 g day^{-1} in countries such as Zaire and the Democratic Republic of Congo, which is an order of magnitude higher than our assumed daily intake rate. Consumption of contaminated cassava leaves at the observed levels of contamination and at rates of 500 g day^{-1} would surpass RfD levels. Despite the reported health benefits of eating cassava leaves (Latif and Müller, 2014), we suggest dietary caution when consuming cassava foliage grown in close proximity to ASGM, and this likely applies for other edible plant foliage.

Although maize and peanut leaves are not typically consumed by humans, they are frequently used as fodder for livestock (Samkol, 2018; Abdul Rahman et al., 2022). This introduces an additional layer of concern, as the ingestion of Hg-laden plants by livestock can lead to the accumulation of Hg in livestock kidneys and liver (Verman et al, 1986; Crout et al., 2004). Human exposure through the consumption of Hg contaminated meat and dairy/egg products is an additional understudied potential human exposure pathway.

Supplement link

The supplementary information is available at *XXXX* and contains all complementary information and all data used within study as well as extended details on the study methods. No specialised modelling code was used to perform the calculations used and all data can

https://doi.org/10.5194/egusphere-2025-1402
Preprint. Discussion started: 8 April 2025

be recreated from the raw data and equations provided in the supplement.

Author Contributions

E.O.E. built research partnerships in Nigeria, contributed to experimental design, led field work and sample collection, undertook sample preparations and analysis, generated figures, wrote the manuscript draft. N.V. worked on the development of analytical methods (including Hg isotope combust and trap), undertook sample preparation and analysis (including Hg stable isotope analyses in Toulouse), and provided reviews of the manuscript. A.O.M. built connections with Uke community and mining stakeholders, contributed to experimental design and fieldwork, provided lab space for sample preparations at the University of Lagos, and provided reviews of the manuscript. N.C.A. built connections with Uke community and mining stakeholders, contributed to experimental design and fieldwork (including follow-up sampling and MerPAS collections at Farm2), and provided reviews of the manuscript. J.E.S. provided guidance on Hg stable isotope sample extraction methods, led Hg stable isotopes analyses, and provided reviews of the manuscript. S.S.M. undertook all MeHg analyses and provided reviews of the manuscript. D.S.M. conceptualised the study, built research partnerships in Nigeria, worked on the development of analytical methods, contributed to figures, provided manuscript draft guidance, and reviewed the manuscript.

Competing Interests

D.S.M. is a member of the editorial board of the journal *Biogeosciences*. The authors declare that they have no other conflict of interest.

Acknowledgements

We thank the support from Zinariya Kyautar Allah (Mining) Venture Ltd. and the community of Uke, Nigeria for welcoming us into their community and being active and willing contributors to this work. We acknowledge contributions of the Analytical Services Unit (ASU) team at Queen's University (Meesha Thompson, Paula Whitely, Dale Marecak, and Graham Cairns) for their support and feedback on Hg analyses. A big thank you to Dr. Jason Demers and Dr. Bridget Bergquist for their direction and guidance in setting up our lab for Hg stable isotope sample preparations and extractions. We also thank D.K. Olukoya Central Research and Reference Laboratories from the University of Lagos for providing support in sample drying in Nigeria. We acknowledge Dr. Carl Mitchell for providing the use of their MeHg analysis methods to assess MeHg concentrations in plant

https://doi.org/10.5194/egusphere-2025-1402
Preprint. Discussion started: 8 April 2025

and soil samples. Dr. Jerome Chmeleff is thanked for assistance with Hg isotope analyses.

Financial Support

Finally, we acknowledge an internal, alumni-based, graduate scholarship/award (Maria Nathanson/IAMGOLD Fund: 50540) from Queen's University for funding this work.

References

Abdul Rahman, N., Larbi, A., Addah, W., Sulleyman, K. W., Adda, J. K., Kizito, F., and Hoeschle-Zeledon, I.: Optimizing food and feed in maize–livestock systems in northern Ghana: The effect of maize leaf stripping on grain yield and leaf fodder quality, Agriculture, 12, 275, https://doi.org/10.3390/agriculture12020275, 2022.

Achina-Obeng, R., and Aram, S. A.: Informal artisanal and small-scale gold mining (ASGM) in Ghana: Assessing environmental impacts, reasons for engagement, and mitigation strategies, Resour. Policy, 78, 102907, https://doi.org/10.1016/j.resourpol.2022.102907, 2022.

Addai-Arhin, S., Novirsa, R., Jeong, H., Phan, Q. D., Hirota, N., Ishibashi, Y., Shiratsuchi, H., and Arizono, K.: Mercury waste from artisanal and small-scale gold mining facilities: a risk to farm ecosystems—a case study of Obuasi, Ghana, Environ. Sci. Pollut. Res., 30, 4293–4308, https://doi.org/10.1007/s11356-022-22456-4, 2023.

Adjorlolo-Gasokpoh, A., Golow, A. A., and Kambo-Dorsa, J.: Mercury in the surface soil and cassava, Manihot esculenta (flesh, leaves, and peel) near goldmines at Bogoso and Prestea, Ghana, Bull. Environ. Contam. Toxicol., 89, 1106–1110, https://doi.org/10.1007/s00128-012-0849-7, 2012.

Afandi, Y., Tejowulan, R. S., and Baiq, D. K.: Mercury uptake by Zea mays L. grown on an inceptisol polluted by amalgamation and cyanidation tailings of small-scale gold mining, J. Degrad. Min. Lands Manag., 6, 1821, https://doi.org/10.15243/jdmlm.2019.063.1821, 2019.

Ariya, P. A., Amyot, M., Dastoor, A., Deeds, D., Feinberg, A., Kos, G., Poulain, A., Ryjkov, A., Semeniuk, K., Subir, M., and Toyota, K.: Mercury physicochemical and biogeochemical transformation in the atmosphere and at atmospheric interfaces: a review and future directions, Chem. Rev., 115, 3760–3802, https://doi.org/10.1021/cr500667e, 2015.

Assad, M., Parelle, J., Cazaux, D., Gimbert, F., Chalot, M., and Tatin-Froux, F.: Mercury uptake into

https://doi.org/10.5194/egusphere-2025-1402
Preprint. Discussion started: 8 April 2025

549 poplar leaves, Chemosphere, 146, 1–7, https://doi.org/10.1016/j.chemosphere.2015.11.103, 2016.

550 Basu, N., Bastiansz, A., Dórea, J. G., Fujimura, M., Horvat, M., Shroff, E., Weihe, P., and Zastenskaya,
551 I.: Our evolved understanding of the human health risks of mercury, Ambio, 52, 877–896,
552 https://doi.org/10.1007/s13280-023-01831-6, 2023.

553 Basuchaudhuri, P.: Physiology of the Peanut Plant, CRC Press, Boca Raton, USA, p. 430,
554 https://doi.org/10.1201/9781003262220, 2022.

555 Bergquist, B. A., and Blum, J. D.: Mass-dependent and -independent fractionation of Hg isotopes by
556 photoreduction in aquatic systems, Science, 318, 417–420,
557 https://doi.org/10.1126/science.1148050, 2007.

558 Bergquist, B. A., and Blum, J. D.: The odds and evens of mercury isotopes: applications of mass-
559 dependent and mass-independent isotope fractionation, Elements, 5, 353–357,
560 https://doi.org/10.2113/gselements.5.6.353, 2009.

561 Biester, H., and Scholz, C.: Determination of mercury binding forms in contaminated soils: mercury
562 pyrolysis versus sequential extractions, Environ. Sci. Technol., 31, 233–239,
563 https://doi.org/10.1021/es960369h, 1996.

564 Blum, J. D., and Bergquist, B. A.: Reporting of variations in the natural isotopic composition of
565 mercury, Anal. Bioanal. Chem., 388, 353–359, https://doi.org/10.1007/s00216-007-1236-9, 2007.

566 Bose-O'Reilly, S., Drasch, G., Beinhoff, C., Rodrigues-Filho, S., Roider, G., Lettmeier, B., Maydl, A.,
567 Maydl, S., and Siebert, U.: Health assessment of artisanal gold miners in Indonesia, Sci. Total
568 Environ., 408, 713–725, https://doi.org/10.1016/j.scitotenv.2009.10.070, 2009.

569 Bräutigam, A., and Gowik, U.: Photorespiration connects C3 and C4 photosynthesis, J. Exp. Bot., 67,
570 2953–2962, https://doi.org/10.1093/jxb/erw056, 2016.

571 Browne, C. L., and Fang, S. C.: Differential uptake of mercury vapor by gramineous C3 and C4 plants,
572 Plant Physiol., 72, 1040–1042, https://doi.org/10.1104/pp.72.4.1040, 1983.

573 Bugmann, A., Brugger, F., Zongo, T., and Van der Merwe, A.: "Doing ASGM without mercury is like
574 trying to make omelets without eggs": Understanding the persistence of mercury use among
575 artisanal gold miners in Burkina Faso, Environ. Sci. Policy, 133, 87–97,
576 https://doi.org/10.1016/j.envsci.2022.03.009, 2022.

https://doi.org/10.5194/egusphere-2025-1402
Preprint. Discussion started: 8 April 2025

577 Casagrande, G. C. R., Franco, D. N. D. M., Moreno, M. I. C., de Andrade, E. A., Battirola, L. D., and de
578 Andrade, R. L. T.: Assessment of atmospheric mercury deposition in the vicinity of artisanal and
579 small-scale gold mines using Glycine max as bioindicators, Water Air Soil Pollut., 231, 1–14,
580 https://doi.org/10.1007/s11270-020-04918-y, 2020.

581 Castilhos, Z. C., and Domingos, L. M. B.: A picture of artisanal and small-scale gold mining (ASGM)
582 in Brazil and its mercury emissions and releases, Environ. Geochem. Health, 46, 101,
583 https://doi.org/10.1007/s10653-024-01881-z, 2024.

584 Cobbina, S. J., Duwiejuah, A. B., and Quainoo, A. K.: Single and simultaneous adsorption of heavy
585 metals onto groundnut shell biochar produced under fast and slow pyrolysis, Int. J. Environ. Sci.
586 Technol., 16, 3081–3090, https://doi.org/10.1007/s13762-018-1910-9, 2019.

587 Crout, N. M. J., Beresford, N. A., Dawson, J. M., Soar, J., and Mayes, R. W.: The transfer of 73As, 109Cd
588 and 203Hg to the milk and tissues of dairy cattle, J. Agr. Sci., 142, 203–212,
589 https://doi.org/10.1017/S0021859604004186, 2004.

590 Cui, L., Feng, X., Lin, C. J., Wang, X., Meng, B., Wang, X., and Wang, H.: Accumulation and
591 translocation of 198Hg in four crop species, Environ. Toxicol. Chem., 33, 334–340,
592 https://doi.org/10.1002/etc.2443, 2014.

593 Demers, J. D., Blum, J. D., and Zak, D. R.: Mercury isotopes in a forested ecosystem: Implications for
594 air-surface exchange dynamics and the global mercury cycle, Global Biogeochem. Cy., 27, 222–238,
595 https://doi.org/10.1002/gbc.20021, 2013.

596 El-Sharkawy, M. A.: Cassava biology and physiology, Plant Mol. Biol., 53, 621–641,
597 https://doi.org/10.1023/B:PLAN.0000019109.01740.c6, 2003.

598 El-Sharkawy, M. A. and Cock, J. H.: C3-C4 intermediate photosynthetic characteristics of cassava
599 (Manihot esculenta Crantz) I. Gas exchange, Photosynth. Res., 12, 219–235,
600 https://doi.org/10.1007/BF00055122, 1987.

601 Enrico, M., Roux, G. L., Marusczak, N., Heimbürger, L., Claustres, A., Fu, X., Sun, R., and Sonke, J. E.:
602 Atmospheric mercury transfer to peat bogs dominated by gaseous elemental mercury dry
603 deposition, Environ. Sci. Technol., 50, 2405–2412, https://doi.org/10.1021/acs.est.5b06058, 2016.

604 Enrico, M., Balcom, P., Johnston, D. T., Foriel, J., and Sunderland, E. M.: Simultaneous combustion

https://doi.org/10.5194/egusphere-2025-1402
Preprint. Discussion started: 8 April 2025

preparation for mercury isotope analysis and detection of total mercury using a direct mercury analyzer, Anal. Chim. Acta, 1154, 338327, https://doi.org/10.1016/j.aca.2021.338327, 2021.

Estrade, N., Carignan, J., and Donard, O. F.: Tracing and quantifying anthropogenic mercury sources in soils of northern France using isotopic signatures, Environ. Sci. Technol., 45, 1235–1242, https://doi.org/10.1021/es1026823, 2011.

Fu, X., Zhu, W., Zhang, H., Sommar, J., Yu, B., Yang, X., Wang, X., Lin, C., and Feng, X.: Depletion of atmospheric gaseous elemental mercury by plant uptake at Mt. Changbai, Northeast China, Atmos. Chem. Phys., 16, 12861–12873, https://doi.org/10.5194/acp-16-12861-2016, 2016.

Fu, X., Liu, C., Zhang, H., Xu, Y., Zhang, H., Li, J., Lyu, X., Zhang, G., Guo, H., Wang, X., Zhang, L., and Feng, X.: Isotopic compositions of atmospheric total gaseous mercury in 10 Chinese cities and implications for land surface emissions, Atmos. Chem. Phys., 21, 6721–6734, https://doi.org/10.5194/acp-21-6721-2021, 2021.

Gerson, J. R., Szponar, N., Zambrano, A. A., Bergquist, B., Broadbent, E., Driscoll, C. T., Erkenswick, G., Evers, D. C., Fernandez, L. E., Hsu-Kim, H., Inga, G., Lansdale, K. N., Marchese, M. J., Martinez, A., Moore, C., Pan, W. K., Purizaca, R. P., Sánchez, V., Silman, M., Ury, E. A., Vega, C., Watsa, M., and Bernhardt, E. S.: Amazon forests capture high levels of atmospheric mercury pollution from artisanal gold mining, Nat. Commun., 13, https://doi.org/10.1038/s41467-022-27997-3, 2022.

Glauser, E., Wohlgemuth, L., Conen, F., and Jiskra, M.: Total mercury accumulation in aboveground parts of maize plants (Zea mays) throughout a growing season, J. Plant Interact., 17, 239–243, https://doi.org/10.1080/17429145.2022.2028914, 2022.

González-Carrasco, V., Velasquez-Lopez, P. C., Olivero-Verbel, J., and Pájaro-Castro, N.: Air mercury contamination in the gold mining town of Portovelo, Ecuador, Bull. Environ. Contam. Toxicol., 87, 250–253, https://doi.org/10.1007/s00128-011-0345-5, 2011.

Gratz, L. E., Keeler, G. J., Blum, J. D., and Sherman, L. S.: Isotopic composition and fractionation of mercury in Great Lakes precipitation and ambient air, Environ. Sci. Technol., 44, 7764–7770, https://doi.org/10.1021/es100383w, 2010.

Greger, M., Wang, Y., and Neuschütz, C.: Absence of Hg transpiration by shoot after Hg uptake by roots of six terrestrial plant species, Environ. Pollut., 134, 201–208, https://doi.org/10.1016/j.envpol.2004.08.007, 2005.

https://doi.org/10.5194/egusphere-2025-1402
Preprint. Discussion started: 8 April 2025

634 Ha, E., Basu, N., Bose-O'Reilly, S., Dórea, J. G., McSorley, E., Sakamoto, M., and Chan, H. M.: Current
635 progress on understanding the impact of Mercury on human health, Environ. Res., 152, 419–433,
636 https://doi.org/10.1016/j.envres.2016.06.042, 2017.

637 Hinton, J., Veiga, M. M., and Veiga, A.: Clean artisanal gold mining: a utopian approach?, J. Clean.
638 Prod., 11, 99–115, https://doi.org/10.1016/s0959-6526(02)00031-8, 2003.

639 Jiskra, M., Sonke, J. E., Obrist, D., Bieser, J., Ebinghaus, R., Myhre, C. L., Pfaffhuber, K. A., Wängberg,
640 I., Kyllönen, K., Worthy, D., Martin, L. G., Labuschagne, C., Mkololo, T., Ramonet, M., Magand, O., and
641 Dommergue, A.: A vegetation control on seasonal variations in global atmospheric mercury
642 concentrations, Nat. Geosci., 11, 244–250, https://doi.org/10.1038/s41561-018-0078-8, 2018.

643 Jiskra, M., Wiederhold, J. G., Skyllberg, U., Kronberg, R. M., Hajdas, I., and Kretzschmar, R.: Mercury
644 deposition and re-emission pathways in boreal forest soils investigated with Hg isotope signatures,
645 Environ. Sci. Technol., 49, 7188–7196, https://doi.org/10.1021/acs.est.5b00742, 2015.

646 Jønsson, J. B., Charles, E., and Kalvig, P.: Toxic mercury versus appropriate technology: Artisanal gold
647 miners' retort aversion, Resour. Policy, 38, 60–67, https://doi.org/10.1016/j.resourpol.2012.09.001,
648 2013.

649 Kawakami, T., Konishi, M., Imai, Y., and Soe, P. S.: Diffusion of mercury from artisanal small-scale
650 gold mining (ASGM) sites in Myanmar, GEOMATE J., 17, 228–235,
651 https://doi.org/10.21660/2019.61.4823, 2019.

652 Laacouri, A., Nater, E. A., and Kolka, R. K.: Distribution and uptake dynamics of mercury in leaves of
653 common deciduous tree species in Minnesota, USA, Environ. Sci. Technol., 47, 10462–10470,
654 https://doi.org/10.1021/es401357z, 2013.

655 Latif, S., and Müller, J.: Potential of cassava leaves in human nutrition: A review, Trends Food Sci.
656 Technol., 44, 147–158, https://doi.org/10.1016/j.tifs.2015.04.006, 2015.

657 Lewis, D., McNeill, R., and Shabalala, Z.: Gold worth billions smuggled out of Africa, Reuters,
658 https://www.reuters.com/article/us-gold-africa-smuggling-exclusive-idUSKCN1S00V4 (last access:
659 11 November 2023), 2019.

660 Liu, Y., Lin, C. J., Yuan, W., Lu, Z., and Feng, X.: Translocation and distribution of mercury in biomasses
661 from subtropical forest ecosystems: Evidence from stable mercury isotopes, Acta Geochim., 40, 42–

https://doi.org/10.5194/egusphere-2025-1402
Preprint. Discussion started: 8 April 2025

50, https://doi.org/10.1007/s11631-020-00441-3, 2021.

Liu, Y., Sun, X., and Li, B.: Adsorption of Hg^{2+} and Cd^{2+} by ethylenediamine modified peanut shells, Carbohydr. Polym., 81, 335–339, https://doi.org/10.1016/j.carbpol.2010.02.020, 2010.

Lomonte, C., Wang, Y., Doronila, A., Gregory, D., Baker, A. J., Siegele, R., and Kolev, S. D.: Study of the spatial distribution of mercury in roots of vetiver grass (Chrysopogon zizanioides) by micro-PIXE spectrometry, Int. J. Phytoremediat., 16, 1170–1182, https://doi.org/10.1080/15226514.2013.821453, 2014.

Mao, Y., Li, Y., Richards, J., and Cai, Y.: Investigating uptake and translocation of mercury species by sawgrass (Cladium jamaicense) using a stable isotope tracer technique, Environ. Sci. Technol., 47, 9678–9684, https://doi.org/10.1021/es400546s, 2013.

Marshall, B., Camacho, A. A., Jimenez, G., and Veiga, M. M.: Mercury challenges in Mexico: regulatory, trade and environmental impacts, Atmosphere, 12, 57, https://doi.org/10.3390/atmos12010057, 2020.

Mashyanov, N. R., Pogarev, S. E., Panova, E. G., Panichev, N., and Ryzhov, V.: Determination of mercury thermospecies in coal, Fuel, 203, 973–980, https://doi.org/10.1016/j.fuel.2017.03.085, 2017.

McLagan, D. S., Mitchell, C. P., Huang, H., Lei, Y. D., Cole, A. S., Steffen, A., Hung, H., and Wania, F.: A high-precision passive air sampler for gaseous mercury, Environ. Sci. Technol. Lett., 3, 24–29, https://doi.org/10.1021/acs.estlett.5b00319, 2016

McLagan, D. S., Monaci, F., Huang, H., Lei, Y. D., Mitchell, C. P., and Wania, F.: Characterization and quantification of atmospheric mercury sources using passive air samplers, J. Geophys. Res.-Atmos., 124, 2351–2362, https://doi.org/10.1029/2018JD029373, 2019.

McLagan, D. S., Biester, H., Navrátil, T., Kraemer, S. M., and Schwab, L.: Internal tree cycling and atmospheric archiving of mercury: examination with concentration and stable isotope analyses, Biogeosciences, 19, 4415–4429, https://doi.org/10.5194/bg-19-4415-2022, 2022a.

McLagan, D. S., Schwab, L., Wiederhold, J. G., Chen, L., Pietrucha, J., Kraemer, S. M., and Biester, H.: Demystifying mercury geochemistry in contaminated soil–groundwater systems with

https://doi.org/10.5194/egusphere-2025-1402
Preprint. Discussion started: 8 April 2025

690 complementary mercury stable isotope, concentration, and speciation analyses, Environ. Sci.-
691 Process Impacts, 24, 1406–1429, https://doi.org/10.1039/D1EM00368B, 2022b.

692 Millhollen, A. G., Gustin, M. S., and Obrist, D.: Foliar mercury accumulation and exchange for three
693 tree species, Environ. Sci. Technol., 40, 6001–6006, https://doi.org/10.1021/es0609194, 2006.

694 Mitchell, C. P., and Gilmour, C. C.: Methylmercury production in a Chesapeake Bay salt marsh, J.
695 Geophys. Res.-Biogeosci., 113, G2, https://doi.org/10.1029/2008JG000765, 2008.

696 Molina, J. A., Oyarzun, R., and Esbrí, J. M.: Mercury accumulation in soils and plants in the Almadén
697 mining district, Spain: one of the most contaminated sites on Earth, Environ. Geochem. Health, 28,
698 487–498, https://doi.org/10.1007/s10653-006-9058-9, 2006.

699 Moreno-Brush, M., McLagan, D. S., and Biester, H.: Fate of mercury from artisanal and small-scale
700 gold mining in tropical rivers: Hydrological and biogeochemical controls. A critical review, Crit. Rev.
701 Environ. Sci. Technol., 50, 437–475, https://doi.org/10.1080/10643389.2019.1629793, 2020.

702 Munthe, J., Kindbom, K., Parsmo, R., and Yaramenka, K.: Technical Background Report to the Global
703 Mercury Assessment 2018, United Nations Environmental Programme (UNEP), Kenya,
704 https://www.unep.org/globalmercurypartnership/resources/report/technical-background-report-
705 global-mercury-assessment-2018 (last access: 24 June 2024), 2019.

706 Nakazawa, K., Nagafuchi, O., Kawakami, T., Inoue, T., Elvince, R., Kanefuji, K., Nur, I., Napitupulu, M.,
707 Basir-Cyio, M., Kinoshita, H., and Shinozuka, K.: Human health risk assessment of atmospheric
708 mercury inhalation around three artisanal small-scale gold mining areas in Indonesia, Environ. Sci.:
709 Atmos., 1, 423–433, https://doi.org/10.1039/D0EA00019A, 2021.

710 Namasivayam, C., and Periasamy, K.: Bicarbonate-treated peanut hull carbon for mercury (II)
711 removal from aqueous solution, Water Res., 27, 1663–1668, https://doi.org/10.1016/0043-
712 1354(93)90130-A, 1993.

713 Niu, Z., Zhang, X., Wang, Z., and Ci, Z.: Field controlled experiments of mercury accumulation in
714 crops from air and soil, Environ. Pollut., 159, 2684–2689,
715 https://doi.org/10.1016/j.envpol.2011.05.029, 2011.

716 Nyanza, E. C., Dewey, D., Thomas, D. S., Davey, M., and Ngallaba, S. E.: Spatial distribution of
717 mercury and arsenic levels in water, soil and cassava plants in a community with long history of gold

https://doi.org/10.5194/egusphere-2025-1402
Preprint. Discussion started: 8 April 2025

718 mining in Tanzania, Bull. Environ. Contam. Toxicol., 93, 716–721, https://doi.org/10.1007/s00128-
719 014-1315-5, 2014.

720 Obrist, D., Agnan, Y., Jiskra, M., Olson, C. L., Colegrove, D. P., Hueber, J., Moore, C. W., Sonke, J. E.,
721 and Helmig, D.: Tundra uptake of atmospheric elemental mercury drives Arctic mercury pollution,
722 Nature, 547, 201–204, https://doi.org/10.1038/nature22997, 2017.

723 Obrist, D., Roy, E. M., Harrison, J. L., Kwong, C. F., Munger, J. W., Moosmüller, H., Romero, C. D., Sun,
724 S., Zhou, J., and Commane, R.: Previously unaccounted atmospheric mercury deposition in a
725 midlatitude deciduous forest, P. Natl. Acad. Sci. USA, 118, e2105477118,
726 https://doi.org/10.1073/pnas.2105477118, 2021.

727 Odukoya, A. M., Uruowhe, B., Watts, M. J., Hamilton, E. M., Marriott, A. L., Alo, B., and Anene, N. C.:
728 Assessment of bioaccessibility and health risk of mercury within soil of artisanal gold mine sites,
729 Niger, North-central part of Nigeria, Environ. Geochem. Health, 44, 893-909,
730 https://doi.org/10.1007/s10653-021-00991-2, 2022.

731 PlanetGOLD: 2022 Global Forum on Artisanal & Small-Scale Gold Mining,
732 https://www.planetgold.org/2022-global-forum-artisanal-small-scale-gold-mining, last access: 21
733 Oct 2024.

734 Qiu, G., Feng, X., Li, P., Wang, S., Li, G., Shang, L., and Fu, X.: Methylmercury accumulation in rice
735 (Oryza sativa L.) grown at abandoned mercury mines in Guizhou, China, J. Agric. Food Chem., 56,
736 2465–2468, https://doi.org/10.1021/jf073391a, 2008.

737 Rea, A. W., Lindberg, S. E., and Keeler, G. J.: Assessment of dry deposition and foliar leaching of
738 mercury and selected trace elements based on washed foliar and surrogate surfaces, Environ. Sci.
739 Technol., 34, 2418–2425, https://doi.org/10.1021/es991305k, 2000.

740 Rees, D., Westby, A., Tomlins, K., Van Oirschot, Q., Cheema, M. U., Cornelius, E., and Amjad, M.:
741 Tropical root crops, in: Crop Post-Harvest: Science and Technology: Perishables, edited by: Rees, D.,
742 Farrell, G., and Orchard, J., Wiley-Blackwell Publishing, Susse, UK, 392–413,
743 https://doi.org/10.1002/9781444354652.ch18, 2012.

744 Rose, C. H., Ghosh, S., Blum, J. D., and Bergquist, B. A.: Effects of ultraviolet radiation on mercury
745 isotope fractionation during photo-reduction for inorganic and organic mercury species, Chem.
746 Geol., 405, 102–111, https://doi.org/10.1016/j.chemgeo.2015.02.025, 2015.

https://doi.org/10.5194/egusphere-2025-1402
Preprint. Discussion started: 8 April 2025

747 Rutter, A. P., Schauer, J. J., Shafer, M. M., Creswell, J. E., Olson, M. R., Robinson, M., Collins, R. M.,
748 Parman, A. M., Katzman, T. L., and Mallek, J. L.: Dry deposition of gaseous elemental mercury to
749 plants and soils using mercury stable isotopes in a controlled environment, Atmos. Environ., 45, 848–
750 855, https://doi.org/10.1016/j.atmosenv.2010.11.025, 2011a.

751 Rutter, A. P., Schauer, J. J., Shafer, M. M., Creswell, J., Olson, M. R., Clary, A., Robinson, M., Parman,
752 A. M., and Katzman, T. L.: Climate sensitivity of gaseous elemental mercury dry deposition to plants:
753 Impacts of temperature, light intensity, and plant species, Environ. Sci. Technol., 45, 569–575,
754 https://doi.org/10.1021/es102687b, 2011b.

755 Samkol, P.: Groundnut foliage as feed for Cambodian cattle, PhD thesis, Acta Univ. Agric. Sueciae,
756 201:26, 1–50, https://core.ac.uk/download/pdf/211564208.pdf (last access: 21 Dec 2024), 2018.

757 Seccatore, J., Veiga, M., Origliasso, C., Marin, T., and De Tomi, G.: An estimation of the artisanal small-
758 scale production of gold in the world, Sci. Total Environ., 496, 662–667,
759 https://doi.org/10.1016/j.scitotenv.2014.05.003, 2014.

760 Si, M., McLagan, D. S., Mazot, A., Szponar, N., Bergquist, B., Lei, Y. D., Mitchell, C. P. J., and Wania, F.:
761 Measurement of atmospheric mercury over volcanic and fumarolic regions on the North Island of
762 New Zealand using passive air samplers, ACS Earth Space Chem., 4, 2435–2443,
763 https://doi.org/10.1021/acsearthspacechem.0c00274, 2020.

764 Snow, M. A., Darko, G., Gyamfi, O., Ansah, E., Breivik, K., Hoang, C., Lei, Y. D., and Wania, F.:
765 Characterization of inhalation exposure to gaseous elemental mercury during artisanal gold mining
766 and e-waste recycling through combined stationary and personal passive sampling, Environ. Sci.:
767 Process. Impacts, 23, 569–579, https://doi.org/10.1039/d0em00494d, 2021.

768 Sonke, J. E., Schäfer, J., Chmeleff, J., Audry, S., Blanc, G., and Dupré, B.: Sedimentary mercury stable
769 isotope records of atmospheric and riverine pollution from two major European heavy metal
770 refineries, Chem. Geol., 279, 90-100, https://doi.org/10.1016/j.chemgeo.2010.09.017, 2010.

771 Sprovieri, F., Pirrone, N., Bencardino, M., D'Amore, F., Carbone, F., Cinnirella, S., Mannarino, V.,
772 Landis, M., Ebinghaus, R., Weigelt, A., Brunke, E., Labuschagne, C., Martin, L., Munthe, J., Wängberg,
773 I., Artaxo, P., Morais, F., De Melo Jorge Barbosa, H., Brito, J., Cairns, W., Barbante, C., del Carmen
774 Diéguez, M., Garcia, P. E., Dommergue, A., Angot, H., Magand, O., Skov, H., Horvat, M., Kotnik, J.,
775 Read, K. A., Mendes Neves, L., Gawlik, B. M., Sena, F., Mashyanov, N., Obolkin, V., Wip, D., Feng, X.

https://doi.org/10.5194/egusphere-2025-1402
Preprint. Discussion started: 8 April 2025

776 B., Zhang, H., Fu, X., Ramachandran, R., Cossa, D., Knoery, J., Marusczak, N., Nerentorp, M., and
777 Norstrom, C.: Atmospheric mercury concentrations observed at ground-based monitoring sites
778 globally distributed in the framework of the GMOS network, Atmos. Chem. Phys., 16, 11915-11935,
779 https://doi.org/10.5194/acp-16-11915-2016, 2016.

780 Streets, D. G., Horowitz, H. M., Lü, Z., Levin, L., Thackray, C. P., and Sunderland, E. M.: Global and
781 regional trends in mercury emissions and concentrations, 2010–2015, Atmos. Environ., 201, 417-
782 427, https://doi.org/10.1016/j.atmosenv.2018.12.031, 2019.

783 Suhadi, S., Sueb, S., Muliya, B. K., and Ashoffi, A. M.: Pollution of mercury and cyanide in soils and
784 plants surrounding the Artisanal and Small-Scale Gold Mining (ASGM) at Sekotong District, West
785 Lombok, West Nusa Tenggara, Biol. Environ. Pollut., 1, 30-37,
786 https://doi.org/10.31763/bioenvipo.v1i1.392, 2021.

787 Sun, G., Feng, X., Yin, R., Zhao, H., Zhang, L., Sommar, J., Li, Z., and Zhang, H.: Corn (Zea mays L.): A
788 low methylmercury staple cereal source and an important biospheric sink of atmospheric mercury,
789 and health risk assessment, Environ. Int., 131, 104971,
790 https://doi.org/10.1016/j.envint.2019.104971, 2019.

791 Sun, T., Wang, Z., Zhang, X., Niu, Z., and Chen, J.: Influences of high-level atmospheric gaseous
792 elemental mercury on methylmercury accumulation in maize (Zea mays L.), Environ. Pollut., 265,
793 114890, https://doi.org/10.1016/j.envpol.2020.114890, 2020.

794 Szponar, N., McLagan, D. S., Kaplan, R. J., Mitchell, C. P. J., Wania, F., Steffen, A., Stupple, G. W.,
795 Monaci, F., and Bergquist, B. A.: Isotopic characterization of atmospheric gaseous elemental
796 mercury by passive air sampling, Environ. Sci. Technol., 54, 10533-10543,
797 https://doi.org/10.1021/acs.est.0c02251, 2020.

798 Szponar, N., Su, Y., Stupple, G., McLagan, D. S., Pilote, M., Munoz, A., Mitchell, C. P. J., Steffen, A.,
799 Wania, F., and Bergquist, B. A.: Applying passive air sampling and isotopic characterization to assess
800 spatial variability of gaseous elemental mercury across Ontario, Canada, J. Geophys. Res.-Atmos.,
801 128, e2022JD037361, https://doi.org/10.1029/2022JD037361, 2023.

802 Szponar, N., Vega, C. M., Gerson, J. R., McLagan, D. S., Pillaca, M., Antoni, S., Lee, D., Rahman, N.,
803 Fernandez, L., Bernhardt, E., Kiefer, A., Mitchell, C. P. J., Wania, F., and Bergquist, B.: Tracing
804 atmospheric mercury from artisanal and small-scale gold mining, Environ. Sci. Technol., 59, 5021-

https://doi.org/10.5194/egusphere-2025-1402
Preprint. Discussion started: 8 April 2025

5033, https://doi.org/10.1021/acs.est.4c10521, 2025.

Tang, X., Wang, Y., Ding, C., Yin, Y., Zhou, Z., Zhang, T., and Wang, X.: Cadmium found in peanut (Arachis hypogaea L.) kernels mainly originates from root uptake rather than shell absorption from soil, Pedosphere, 34, 726-735, https://doi.org/10.1016/j.pedsph.2023.05.009, 2024.

Telmer, K. H. and Veiga, M. M.: World emissions of mercury from artisanal and small-scale gold mining, in: Mercury Fate and Transport in the Global Atmosphere: Emissions, Measurements and Models, Springer, Boston, USA, 131-172, https://doi.org/10.1007/978-0-387-93958-2_6, 2009.

Turgeon, R.: Phloem loading: how leaves gain their independence, BioScience, 56, 15-24, https://doi.org/10.1641/0006-3568(2006)056[0015:PLHLGT]2.0.CO;2, 2006.

UNEP: Minamata Convention on Mercury, United Nations Environmental Programme, Kenya, NGA, https://www.unep.org/resources/report/minamata-convention-mercury (last access: 24 June 2024), 2013.

USEPA: Integrated Risk Information System. Methylmercury (MeHg) (CASRN 22967-92-6), US Environmental Protection Agency, Washington, DC, USA, https://cfpub.epa.gov/ncea/iris/iris_documents/documents/subst/0073_summary.pdf (last access: 17 March 2024), 2001.

USEPA: Method 7473: Mercury in solids and Solutions by Thermal Decomposition, Amalgamation, and Atomic Absorption Spectro-Photometry. Test methods for evaluating solid wastes. Physical/Chemical Methods. SW-846 On-Line, United States Environmental Protection Agency (UNEP), Washington, DC, USA, https://www.epa.gov/sites/default/files/2015-12/documents/7473.pdf, 2007.

USEPA: Operating Procedure: Soil Sampling, US Environmental Protection Agency (USEPA), Washington, DC, USA, https://www.epa.gov/sites/production/files/2015-06/documents/Soil-Sampling.pdf, 2023.

Veiga, M. M., Maxson, P. A., and Hylander, L. D.: Origin and consumption of mercury in small-scale gold mining, J. Clean. Prod., 14, 436–447, https://doi.org/10.1016/j.jclepro.2004.08.010, 2006.

Verbrugge, B., and Geenen, S.: The gold commodity frontier: A fresh perspective on change and diversity in the global gold mining economy, Extr. Ind. Soc., 6, 413-423,

https://doi.org/10.5194/egusphere-2025-1402
Preprint. Discussion started: 8 April 2025

https://doi.org/10.1016/j.exis.2018.10.014, 2019.

Verité Inc.: The Nexus of Illegal Gold Mining and Human Trafficking in Global Supply Chains. Lessons from Latin America, Verité Inc. on behalf of Global Initiative Against Transnational Organized Crime, Northampton, USA, https://globalinitiative.net/wp-content/uploads/2018/01/The-nexus-of-illegal-gold-mining.pdf, 2016.

Vreman, K., Van Der Veen, N. G., Van der Molen, E. J., and De Ruig, W. G.: Transfer of cadmium, lead, mercury and arsenic from feed into milk and various tissues of dairy cows: chemical and pathological data, NJAS, 34, 129-144, https://doi.org/10.18174/njas.v34i2.16799, 1986.

Wang, D., Li, Z., and Wang, Q.: Ecological restoration reduces mercury in corn kernel and the distinction of mercury in corn plants in rural China–A case in Wuchuan mercury mining area, Ecotoxicol. Environ. Saf., 271, 115964, https://doi.org/10.1016/j.ecoenv.2024.115964, 2024.

Wang, X., Yuan, W., Lin, C., Luo, J., Wang, F., Feng, X., Fu, X., and Liu, C.: Underestimated sink of atmospheric mercury in a deglaciated forest chronosequence, Environ. Sci. Technol., 54, 8083-8093, https://doi.org/10.1021/acs.est.0c01667, 2020.

Weinhouse, C., Gallis, J. A., Ortiz, E., Berky, A. J., Morales, A. M., Diringer, S. E., Harrington, J., Bullins, P., Rogers, L., Hare-Grogg, J., Hsu-Kim, H., and Pan, W. K.: A population-based mercury exposure assessment near an artisanal and small-scale gold mining site in the Peruvian Amazon, J. Expo. Sci. Environ. Epidemiol., 31, 126-136, https://doi.org/10.1038/s41370-020-0234-2, 2021.

WHO: Environmental health criteria 101: Methylmercury, World Health Organization, Geneva, CHE, https://apps.who.int/iris/bitstream/handle/10665/38082/9241571012_eng.pdf, 1990.

WHO: Elemental mercury and inorganic mercury compounds: Human health aspects (Concise International Chemical Assessment Document 50), World Health Organization (WHO), Geneva, CHE, https://www.who.int/publications/i/item/elemental-mercury-and-inorganic-mercury-compounds-human-health-aspects, 2003.

World Gold Council: Gold mine production, World Gold Council, https://www.gold.org/goldhub/data/historical-mine-production, 2019.

Xia, Z., Du, Z., Zhou, X., Jiang, S., Zhu, T., Wang, L., Chen, F., Carvalho, L., Zou, M., López-Lavalle, L. a. B., Zhang, X., Xu, L., Wang, Z., Chen, M., Feng, B., Wang, S., Li, M., Li, Y., Wang, H., Liu, S., Bao, Y.,

https://doi.org/10.5194/egusphere-2025-1402
Preprint. Discussion started: 8 April 2025

Zhao, L., Zhang, C., Xiao, J., Guo, F., Shen, X., Lu, C., Qiao, F., Ceballos, H., Yan, H., Zhang, H., He, S., Zhao, W., Wan, Y., Chen, Y., Huang, D., Li, K., Liu, B., Peng, M., Zhang, W., Muller, B., Chen, X., Luo, M.C., Xiao, J., and Wang, W.: Pan-genome and Haplotype Map of Cultivars and Their Wild Ancestors Provides Insights into Selective Evolution of Cassava (Manihot esculentaCrantz), bioRxiv, https://doi.org/10.1101/2023.07.02.546475, 2023.

Yin, R., Feng, X., and Meng, B.: Stable mercury isotope variation in rice plants (Oryza sativa L.) from the Wanshan mercury mining district, SW China, Environ. Sci. Technol., 47, 2238-2245, https://doi.org/10.1021/es304302a, 2013.

Yoshimura, A., Koyo, S., and Veiga, M. M.: Estimation of mercury losses and gold production by Artisanal and Small-Scale Gold Mining (ASGM), J. Sustain. Met., 7, 1045–1059, https://doi.org/10.1007/s40831-021-00394-8, 2021.

Yu, B., Fu, X., Yin, R., Zhang, H., Wang, X., Lin, C., Wu, C., Zhang, Y., He, N., Fu, P., Wang, Z., Shang, L., Sommar, J., Sonke, J. E., Maurice, L., Guinot, B., and Feng, X.: Isotopic composition of atmospheric mercury in China: new evidence for sources and transformation processes in air and in vegetation, Environ. Sci. Technol., 50, 9262-9269, https://doi.org/10.1021/acs.est.6b01782, 2016.

Yuan, W., Wang, X., Lin, C. J., Wu, F., Luo, K., Zhang, H., Lu, Z., and Feng, X.: Mercury uptake, accumulation, and translocation in roots of subtropical forest: implications of global mercury budget, Environ. Sci. Technol., 56, 14154-14165, https://doi.org/10.1021/acs.est.2c04217, 2022.

Zhang, H., Feng, X., Larssen, T., Qiu, G., and Vogt, R. D.: In inland China, rice, rather than fish, is the major pathway for methylmercury exposure, Environ. Health Perspect., 118, 1183-1188, https://doi.org/10.1289/ehp.1001915, 2010.

Zhao, L., Meng, B., and Feng, X.: Mercury methylation in rice paddy and accumulation in rice plant: a review, Ecotoxicol. Environ. Saf., 195, 110462, https://doi.org/10.5194/bg-13-2429-2016, 2020.

Zhao, L., Anderson, C. W., Qiu, G., Meng, B., Wang, D., and Feng, X.: Mercury methylation in paddy soil: source and distribution of mercury species at a Hg mining area, Guizhou Province, China, Biogeosciences, 13, 2429-2440, https://doi.org/10.5194/bg-13-2429-2016, 2016.

Zhao, H., Yan, H., Zhang, L., Sun, G., Li, P., and Feng, X.: Mercury contents in rice and potential health risks across China, Environ. Int., 126, 406-412, https://doi.org/10.1016/j.envint.2019.02.055, 2019.

https://doi.org/10.5194/egusphere-2025-1402
Preprint. Discussion started: 8 April 2025

889 Zhou, J., Obrist, D., Dastoor, A., Jiskra, M., and Ryjkov, A.: Vegetation uptake of mercury and impacts
890 on global cycling, Nat. Rev. Earth Environ., 2, 269-284, https://doi.org/10.1038/s43017-021-00146-y,
891 2021.

892 Zhou, J., and Obrist, D.: Global mercury assimilation by vegetation, Environ. Sci. Technol., 55, 14245–
893 14257, https://doi.org/10.1021/acs.est.1c03530, 2021.